Iron(III)-Mediated Atom Transfer Radical Polymerization in the Absence of Any Additives

Zhigang Xue,[†] Dan He,[†] Seok Kyun Noh,*[,†] and Won Seok Lyoo[‡]

Schools of Display and Chemical Engineering and Textiles, Yeungnam University, 214-1 Daedong, Gyeongsan, Gyeongbook 712-749, South Korea

Received November 20, 2008; Revised Manuscript Received February 23, 2009

ABSTRACT: The pyridylphosphine ligand, 2-(diphenylphosphino)pyridine (DPPP), was employed in the iron(III)-catalyzed atom transfer radical polymerizations (ATRPs) of methyl methacrylate (MMA) with various initiators and solvents in the absence of any radical initiators or reducing agents. In studies of their ATRP behavior, most of these systems were well controlled with a linear increase in the molecular weight (M_n) versus conversion in agreement with the theoretical M_n, and low-molecular-weight distributions ($M_w/M_n = 1.10$ to 1.25) were observed throughout the reactions. The effect of a protic solvent (methanol) was also investigated, and it was shown that living radical polymerization occurred, even in the presence of relatively high concentrations of methanol. The controlled nature of the polymerization was confirmed by the monomer addition experiment and the block copolymerization.

Introduction

Since its discovery in 1995,[1,2] atom transfer radical polymerization (ATRP) has been developed into a versatile tool for obtaining well-defined polymers.[3−7] ATRP is a transition-metal-mediated halide exchange process that establishes a fast and dynamic equilibrium between a low concentration of growing radicals and a large amount of dormant species, which are unable to propagate and self-terminate. Therefore, polymers with predetermined molecular weights (M_n) and narrow molecular weight distributions (M_w/M_n) can be synthesized. The transition-metal complex is composed of a metal halide and a ligand. The catalyst plays an important role in ATRP, and for this purpose, Matyjaszewski, Sawamoto, and others have made a great deal of effort to research the effect of various complexes on polymerization, such as copper,[3−10] iron,[11−28] ruthenium,[11,29−35] and other metals.[36−42] Among these complexes, iron salt-based catalysts have attracted particular attention owing to their low toxicity, low cost, and biocompatibility.

According to published reports, some iron complexes were active catalysts for normal and reverse ATRP of MMA and styrene with various ligands: phosphorus-based ligands,[11,12] pyridylphosphine,[13,14] diimine,[15,16] diamine,[16] tridentate nitrogen ligands,[17] dimino- and diaminopyridine,[18] tris(3,6-dioxaheptyl)-amine,[19] tridentate salicylaldiminato,[20] tetradentate nitrogen ligands,[21] hexamethylphosphoric triamide,[22] trinuclear iron complex,[23] bis(oxazoline),[24] iron imidazolylidene complex,[25] halide anions,[26] carboxylic acid derivatives,[27] and half-metallocene iron iodide complex [Fe(Cp)I(CO)$_2$].[28] In these complexes, metals have low oxidation state in normal ATRP. The addition of a certain amount of metal salt in higher oxidation state has proven to be efficient in improving the controllability of ATRP.[14,43] Very recently, Schubert[44] and coworkers reported that the ATRP of MMA with the use of only copper(II) resulted in well-defined MMA. However, low initiation efficiencies were obtained.

Selecting the correct conditions for initiation of the ATRP reaction is the first step in any well-controlled ATRP. Using air-stable catalysts in their higher oxidation states was successfully developed and used as a tool in preparing well-defined polymers. The use of oxidatively stable catalysts overcomes the air-sensitive problem of lower-oxidation-state metals and makes the preparation and storage of ATRP catalyst systems more facile. In a reverse ATRP, the transition-metal complex in a lower oxidation state and the ATRP initiator are generated in situ by reactions triggered by decomposition of a conventional free radical initiator.[45−47] The simultaneous reverse and normal initiation (SR&NI) in ATRP was developed from the reverse ATRP.[48] In SR&NI, a small amount of low-oxidation-state metal complex is generated by decomposition of a conventional free radical initiator. However, the majority of polymer chains are initiated from an added ATRP initiator. A reducing agent such as tin(II) 2-ethylhexanoate[49] or triethylamine[50] can reduce the higher-oxidation-state transition metal in the activators generated by electron transfer (AGET) ATRP. Compared with the reported reverse ATRP or AGET ATRP, our catalyst system was conducted using only iron(III) in the absence of any additives;[51,52] therefore, the system is less toxic and less expensive, making it attractive for potential practical application.

The role of ligand is to provide the appropriate solubility and an adjustable redox potential for metal complexes.[4] Therefore, ligand design is very important for providing polymer with a narrow molecular weight distribution. A large number of nitrogen-based ligands have been used for ATRP.[3−10] Consequently, the relationship of ligand structure with its effects on catalyst reactivity and controllability of polymerization was studied. Our interest in ATRP is to develop new iron complexes with pyridylphosphine ligands, which are known to act as donor ligands in the coordination chemistry of transition metals, owing to the simultaneous presence of the ubiquitous pyridine and phosphine donor groups.[53] Despite a great deal of studies related to ligand structure, bidentate catalyst systems possessing both phosphorus and nitrogen are rarely studied in ATRP systems. Very recently, we reported that the ATRP of MMA and styrene were successfully performed using pyridylphosphine as the ligand.[13,14] Variation of experimental conditions led to the observation that the ATRP process mediated by $FeBr_2$/pyridylphosphines/BPN yielded polymers with controlled molecular weights and narrow molecular weight distributions ($M_w/M_n = 1.15$ to 1.3). However, the lowest polydispersity (PDI) value for PMMA by $FeBr_2$/pyridylphosphines/EBriB systems was 1.33. In addition, the metal salt in its higher oxidation state is air stable. The effect of iron(III) on ATRP was therefore

* Corresponding author. E-mail: sknoh@ynu.ac.kr.
[†] School of Display and Chemical Engineering.
[‡] School of Textiles.

10.1021/ma802610a CCC: $40.75
Published on Web 03/19/2009

Table 1. Results of Iron-Based Catalysts in ATRP[a]

entry	metal salt	[C]/[L]/[I][b]	time (h)	conv (%)	$M_{n,th}$[c]	$M_{n,GPC}$	PDI	k_{app} ($\times 10^{-5}$, s^{-1})[d]
1	$FeBr_2$	1/2/1	5	82	16 550	17 850	1.37	9.44
2	$FeBr_3$	1/2/1	9	87	17 550	17 500	1.18	6.18
3	$FeBr_3$	1/1/1	6	57	11 700	12 400	1.15	4.06
4	$FeBr_3$	1/2/1	6	74	14 950	14 100	1.20	6.18
5	$FeBr_3$	1/3/1	6	62	12 650	12 250	1.18	4.37
6	$FeBr_3$/$FeBr_2$	0.8/0.2/2/1	6	72	14 600	15 400	1.25	6.05
7	$FeBr_3$/$FeBr_2$	0.5/0.5/2/1	6	75	15 200	15 800	1.26	6.48
8	$FeBr_3$/$FeBr_2$	0.2/0.8/2/1	6	79	16 000	17 400	1.30	6.97
9	$FeBr_3$/Fe	0.66/0.33/2/1	5	80	16 200	17 900	1.26	8.99
10	$FeBr_2$/Fe	1/1/2/1	5	94	19 100	23 700	1.36	16.07
11	Fe	1/2/1	2	20	4200	370 200	1.61	
12	$FeCl_2$	1/2/1	8	83	16 800	17 900	1.35	7.65
13	$FeCl_3$	1/2/1	8	76	15 350	14 500	1.26	5.16
14	$FeCl_3$[e]	1/2/1	9	53	10 800	8800	1.19	2.36
15	$FeBr_3$	1/0/1	30					
16	$FeBr_3$	1/2/0	30	36		179 000	1.30	

[a] $[MMA]_0 = 4.67$ M. [b] C: iron catalyst; L: ligand (DPPP); I: initiator (EBriB). [c] $M_{n,th} = ([MMA]_0/[EBriB]_0)M_{MMA} \times \text{conv}\ (\%) + M_{EBriB}$; M_{MMA} and M_{EBriB} are the molecular weights of the monomer, MMA, and the initiator, EBriB. [d] Slope of $\ln[M]_0/[M]$ versus time plot. [e] Hygroscopic $FeCl_3$.

investigated in detail, and the results are shown herein. In this study, we described an efficient FeX_3/DPPP catalytic system (X = Cl, Br) for ATRP of MMA in the absence of any radical initiator or reducing agent. The effects of solvent and temperature on this type of ATRP are also reported.

Experimental Section

Materials. Methyl methacrylate (MMA, 99%, Aldrich), styrene (99%, Aldrich), and *n*-butyl methacrylate (BMA, 99%, Aldrich) were passed through a column filled with neutral alumina, dried over CaH_2, distilled under reduced pressure, and stored in a freezer under nitrogen. Tetrahydrofuran (THF, HPLC grade, Fisher) and toluene (certified grade, Fisher) were freshly distilled from Na/K alloy with benzophenone (99%, Aldrich) and stored under nitrogen. 2-(Diphenylphosphino)pyridine (DPPP, 97%, Aldrich), triphenylphosphine (TPP, 99%, Aldrich), 2,2′-bipyridyl (bpy, 99+%, Aldrich), *N*,*N*,*N*′,*N*″,*N*″-pentamethyldiethylenetriamine (PMDETA, 99%, Aldrich), 1,1,4,7,10,10-hexamethyltriethylenetetramine (HMTETA, 97%, Aldrich), galvinoxyl (Aldrich), 2,2,6,6-tetramethylpiperidine 1-oxyl (TEMPO, 99%, Aldrich), $FeBr_2$ (98%, Aldrich), $FeCl_2$ (98%, Aldrich), $FeBr_3$ (98%, Aldrich), $FeCl_3$ (97%, Aldrich), $CuBr_2$ (99.999%, Aldrich), ethyl 2-bromoisobutyrate (EBriB, 99%, Aldrich), 2-bromopropionitrile (BPN, 97%, Aldrich), methyl 2-bromopropionate (MBP, 98%, Aldrich), 1-phenylethyl bromide (PEBr, 97%, Aldrich), 1-phenylethyl chloride (PECl, 97%, TCI), diethyl 2-bromo-2-methylmalonate (DEBM, 98%, Aldrich), *p*-xylene (97%, Aldrich), anisole (99%, Aldrich), methanol (MeOH, 99.9+%, Aldrich), methyl ethyl ketone (MEK, 99+%, Aldrich), and all other solvents were used without further purification.

Polymerization Procedures. $FeBr_3$ is very difficult to handle because it is a hygroscopic chemical. The anhydrous $FeBr_3$ was sealed with paraffin under a dry nitrogen atmosphere and saved in glovebox. The polymerization reaction was carried out by the syringe technique under dry nitrogen. A typical example for MMA polymerization is given below. A Schlenk flask (25 mL) was charged with $FeBr_3$ (138.2 mg, 0.467 mmol) and the ligand (yellow solid, 236.2 mg, 0.934 mmol). The flask was sealed with a rubber septum and was cycled three times between vacuum and nitrogen to remove the oxygen. The degassed solvent (4 mL) (in solution polymerization), anisole (1 mL), and monomer (5 mL, 46.7 mmol) were then added to the flask through degassed syringes. The solution was stirred for 20 min at room temperature; then, the desired amount of EBriB (69.3 μL, 0.467 mmol) was added. The flask was sealed with a new rubber septum and degassed by three freeze−pump−thaw cycles to remove the oxygen. The flask was immersed in a thermostatted oil bath. At timed intervals, samples were withdrawn from the flask with a degassed syringe and diluted with THF and then filtered through a column filled with neutral aluminum oxide to remove the iron catalyst. Parts of the polymer solution were used for gas chromatography (GC) measurements to determine the monomer conversions. Other parts of the PMMA solution were then precipitated using an excess of *n*-hexane, and these polymers were dried under vacuum for 24 h in preparation for gel permeation chromatography (GPC) measurements to determine the molecular weights of the polymers. The polymerizations of styrene and copolymerization were carried out using a similar polymerization procedure.

Reaction of MMA with $FeBr_3$. A Schlenk flask (25 mL) was charged with $FeBr_3$ (2.763 mg, 9.34 mmol) and MMA (1 mL, 9.34 mmol). The mixture was freeze−pump−thawed three times and back-filled with dry nitrogen. The flask was immersed in an oil bath preheated to 80 °C. After 48 h, the liquid phases were separated and analyzed by ^{1}H NMR spectroscopy. The ratio of halogenated monomer to MMA was 5:7. The peaks at 1.92 ($-CH_3$), 3.72 ($-OCH_3$), and 5.55 and 6.08 ppm ($>CH_2$) corresponded to MMA, and those at 2.02 ($-CH_3$), 3.81 ($-OCH_3$), and 3.69 and 4.20 ppm ($>CH_2$) corresponded to dibromoisobutyrate.

Measurements. ^{1}H (300 MHz) NMR spectra were obtained on a Bruker DPX-300 FT-NMR spectrometer in $CDCl_3$ solvent. The monomer conversion was determined in THF solvent with anisole as an internal standard with an HP 6890 gas chromatography equipped with an FID detector and a J&W Scientific 30 m DB WAX megabore column. The injector and detector temperatures were kept at 250 °C. The analysis was run isothermally at 40 °C for 1 min, following which the temperature was increased to 120 °C at a heating rate of 20 °C/min and held at this temperature for 1 min before being increased again to 180 °C at a heating rate of 10 °C/min and being held at this temperature for 1 min. The number-average molecular weight and molecular weight distribution (M_w/M_n) of the polymers were determined by GPC using Waters columns (Styragel, HR 5E) equipped with a Waters 515 pump and a Waters 2410 differential refractometer using diphenyl ether as an internal standard. THF was used as the eluent at a flow rate of 1 mL/min. Linear polystyrene standards were used for calibration.

Results and Discussion

Initially, the polymerizations of MMA in toluene at 80 °C were performed using FeX_3/DPPP or FeX_2/DPPP as complex (X = Cl, Br) and EBriB as initiator. Table 1 shows the results of polymerizations of MMA in different catalyst systems.

In the case of polymerizations with $FeBr_2$/DPPP and $FeCl_2$/DPPP, the molecular weights were higher than the predicted values, indicating a lower efficiency of initiation system presumably caused by the slow deactivation. The PDIs were also relatively high (>1.3) (Table 1, entries 1 and 12). The addition of a metal salt in its higher oxidation state has proven to be helpful in improving the controllability of the ATRP system.[43] As expected, increasing the amount of deactivator resulted in polymers with low PDIs (Table 1, entries 6, 7, and

8). In the case of higher amount of $FeBr_3$, lower rate of polymerization was obtained. Besides, the improved control over the molecular weights was achieved. These results obtained for the ATRP of MMA catalyzed by FeX_2/DPPP/EBriB indicated that there was not enough iron(III) generated in redox process to deactivate the radicals to dormant species. In contrast, when adding the metal salt in its higher oxidation state, the radical concentration was reduced, and therefore, the controllability of polymerization was improved.

To our surprise and excitation, the polymerizations of MMA can be controlled very well using only iron(III) in the absence of any additives (Table 1, entries 2, 3, 4, and 5). The monomer conversion reached 87% at a reaction of 9 h in toluene at 80 °C using $FeBr_3$/DPPP system (Table 1, entry 2), and the PDI remained low. In addition, the effect of the ratio of DPPP to $FeBr_3$ was studied (Table 1, entries 3, 4, 5, and 15). The molecular weights matched the theoretical values very well, and low molecular weight distributions ($M_w/M_n = 1.15$ to 1.20) were obtained in all cases. However, in the case in which the polymerization was carried out with a ratio of 3:1 of ligand to metal salt, the polymerization rate was lower than that obtained from a 2:1 ratio. One possible explanation for this is that when the ligand concentration is further increased, the coordination of the ligand to the metal center may hinder the activity of the catalyst.[13,14,54] There was no reaction when the ratio of ligand to $FeBr_3$ was 0:1. The addition of iron powder to salts of iron(II) or iron(III) resulted in a dramatic increase in polymerization rate (Table 1, entries 9 and 10). The PDI of the iron(III)/iron(0) system was a little higher than that of the only iron(III) system. The iron(II)/iron(0) catalyst system provided polymer with a molecular weight higher than that predicted and with a higher polydispersity (PDI = 1.36). Iron(0) only with the ligand also promoted ATRP but with less control over the polymerization (Table 1, entry 11).

Effect of Ligand on ATRP of MMA. In ATRP, choice of ligand is an important research direction because a suitable ligand can lower the redox potential of the metal and improve both activity and controllability of the catalyst. Then, to demonstrate the advantages of the pyridylphosphine ligand (DPPP), the same experiments were performed with the triphenlyphosphine ligand (TPP)/iron(III) system. The structure of DPPP is similar to that of TPP, which was used as a ligand in living radical polymerization by Sawamoto.[3] The ATRP of MMA was performed in toluene at 80 °C using EBriB as initiator and FeX_3 or $CuBr_2$ as catalyst in conjunction with various ligands. The results are illustrated in Figure 1a,b.

The polymerizations of MMA proceeded with first-order kinetics with respect to monomer for FeX_3/DPPP, whereas FeX_3/TPP showed some slight curvatures in the first-order kinetics plot, indicating a detectable termination, as shown in Figure 1a. To see the advantages of a high-oxidation-state metal, the same experiment with $CuBr_2$/HMTETA as complex was run. The straight line passing through the origin indicated that the polymerization proceeded with an approximately constant radical concentration. Moreover, the conversion reached 91% in only 6 h without any loss control, and the molecular weight and its distribution of PMMA obtained from $CuBr_2$/HMTETA were controlled well (PDI = 1.16). The dependence of M_n and M_w/M_n on monomer conversion in different catalyst systems is shown in Figure 1b. In the case of FeX_3/2TPP systems, some deviations of molecular weights and relatively high PDI values (M_w/M_n = 1.2 to 1.35) were observed, and the measured molecular weights were lower than the theoretical values. These results indicated that controllability of the polymerizations was poor, presumably because of the formation of additional polymer chains that could be generated through transfer reactions.[11,55,56] Notably, when the ratio of $FeBr_3$ to TPP was 1:3, molecular

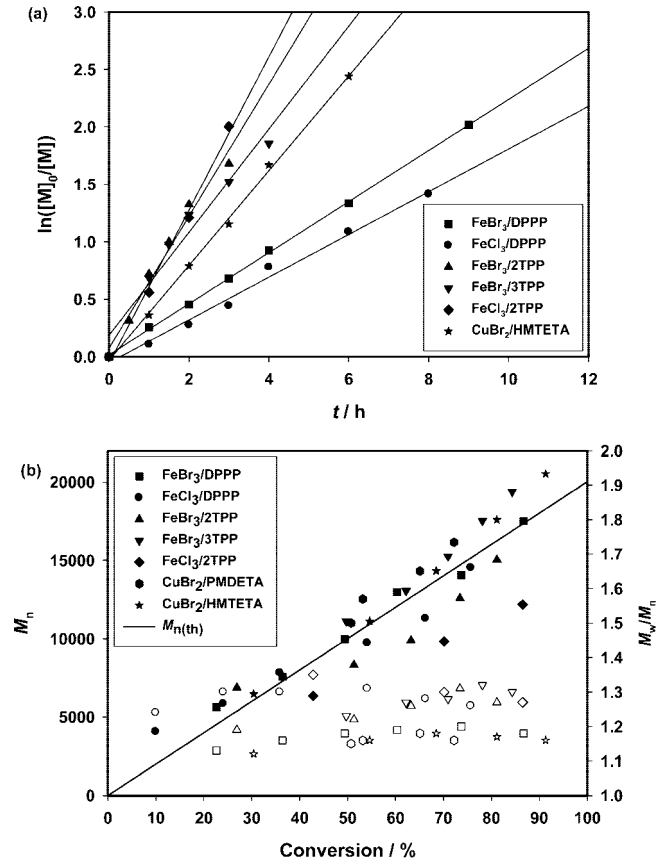

Figure 1. (a) Kinetics plots of $\ln[M]_0/[M]$ versus reaction time and (b) dependence of molecular weights, M_n (filled symbols), and molecular weight distributions, M_w/M_n (open symbols), on the monomer conversion for the ATRP of MMA in toluene with different complexes at 80 °C. $[MMA]_0 = 4.67$ M; $[MMA]_0/[EBriB]_0/[Complex]_0 = 200:1:1$.

weights were slightly higher than the calculated ones, and a slight decrease in the rate of polymerization was observed. One possible explanation for these is that the solubility of the catalyst complex is high at a higher ligand concentration, which makes polymerization easy to be controlled, and other explanations need further study. However, the molecular weights matched the theoretical values better and the molecular weight distributions ($M_w/M_n = 1.13$ to 1.20) were narrower when $FeBr_3$/DPPP was employed instead of $FeBr_3$/TPP. At the same time, we also investigated the ATRP of MMA using various nitrogen ligands in the presence of only $CuBr_2$. $CuBr_2$/PMDETA or $CuBr_2$/HMTETA systems can yield polymers with molecular weights closer to the theoretical values and with low-molecular-weight distributions (M_w/M_n = 1.12 to 1.18). In addition, the rate of polymerization obtained from PMDETA or HMTETA was higher than that with bpy as the ligand, and polydispersities were relatively higher (PDI = 1.18 to 1.35). These might have been due to coordination complexes between copper and simple amines having lower redox potentials and better solubility than the $CuBr_2$/bpy complex.[57]

Effect of Solvent on ATRP of MMA. The ATRP of MMA can be performed either in polar solvent or nonpolar solvent. To investigate the effect of solvent on polymerization of MMA initiated by EBriB and catalyzed by $FeBr_3$/DPPP, a series of solvents were examined. The polymerization of MMA in anisole or MEK proceeded at a faster rate than that in nonpolar solvents such as toluene and *p*-xylene at 80 °C. (See Figure 2a.) This is because increasing the polarity of the solvent can affect the solubility of the catalyst and produce high activity.[58]

Figure 2b shows the plots of M_n and M_w/M_n against the monomer conversion. As shown in Figure 2b, the molecular

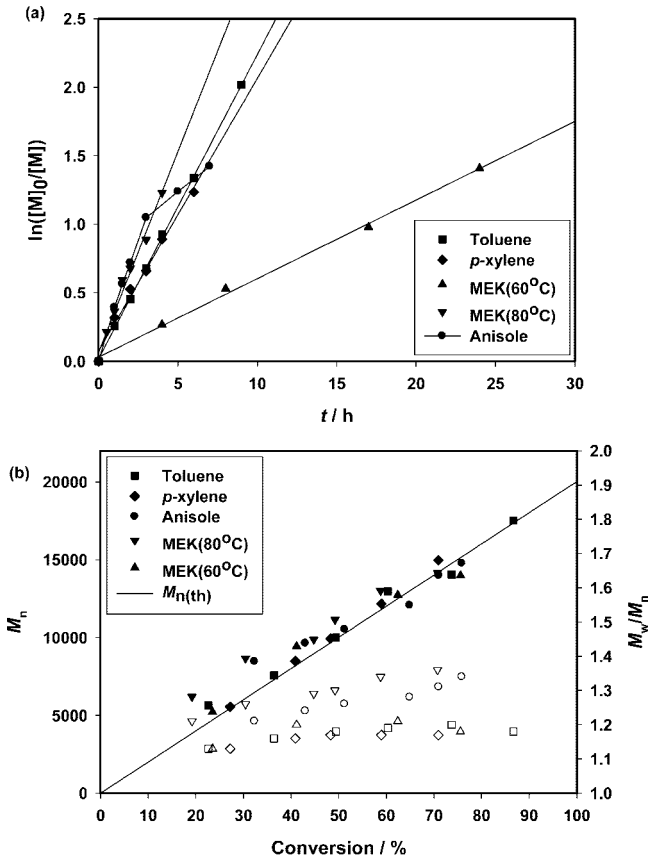

Figure 2. (a) Kinetics plots of $\ln[M]_0/[M]$ versus reaction time and (b) dependence of molecular weights, M_n (filled symbols), and molecular weight distributions, M_w/M_n (open symbols), on the monomer conversion for the ATRP of MMA in different solvent systems at 80 °C. $[MMA]_0 = 4.67$ M; $[MMA]_0/[EBriB]_0/[FeBr_3]_0/[DPPP]_0 = 200:1:1:2$.

weights of PMMA prepared in all of the solvents increased linearly with increasing monomer conversion and followed the theoretical line. The narrow polydispersities were observed ($M_w/M_n < 1.2$) in toluene and *p*-xylene. However, relatively higher PDI values were observed when anisole or MEK was used as the solvent (PDI = 1.21 to 1.34). To minimize side reactions occurring in polar solvent, the polymerization of MMA in MEK was carried out at 60 °C. It gave a linear first-order kinetics plot (Figure 2a), indicating that the polymerization proceeded with an approximately constant number of active species, and termination reactions were not significant. Low polydispersities (M_w/M_n = 1.13 to 1.21) were observed in MEK at 60 °C, whereas at 80 °C, the polydispersities were slightly higher, probably because the thermal acceleration is greater for propagation than for the interconversion rate between the dormant and activated species with temperature.[59]

To examine the effect of protic solvent (MeOH) on polymerization of MMA, a series of polymerizations was performed with $FeBr_3$/DPPP system in mixed toluene/MeOH solutions, and the results are shown in Table 2. As expected, increasing the MeOH concentration led to an enhancement of the polymerization rate. However, the trend of molecular weight was decreasing with increasing concentration of MeOH. The molecular weights were lower than the theoretical values, and a slight increase in PDI was observed, presumably due to the chain transfer reaction during the polymerization.

Effect of Initiator on ATRP of MMA. The choice of the initiator is extremely important in the polymerization of MMA, and fast initiation is required to obtain well-defined polymers with a low PDI.[4] Five different initiators were thus examined for the solution ATRP of MMA, viz. EBriB, BPN, PEBr, MBP, and DEBM, in conjunction with the $FeBr_3$/DPPP catalyst system in toluene at 80 °C, and the obtained results are described in Figure 3.

It was found that the polymerizations of MMA proceeded with first-order kinetics with respect to monomer concentration for all initiation systems, which indicated that the radical concentrations remained constant during the reactions, as shown in Figure 3a. Figure 3b shows the dependence of M_n and M_w/M_n on the monomer conversion with the different initiators. The experimental molecular weights matched the calculated ones better, and the molecular weights distributions (M_w/M_n = 1.08 to 1.18) were narrower when the initiator, BPN or EBriB, was employed instead of DEBM, PEBr, and MBP. In the PEBr and MBP systems, the experimental molecular weights were much higher than the theoretical values, which was indicative of inefficient initiation caused by slow deactivation. However, $FeBr_3$/DPPP can still mediate a controlled MMA polymerization using PEBr or MBP as the initiator despite the low initiator efficiency. It is noteworthy that the experimental molecular weights of PMMA obtained from MBP increased linearly with conversion, and the polydispersities (PDI = 1.17 to 1.33) were still low, indicating that the polymerization was a living process. In the $FeBr_2$/DPPP/MBP system, the polydispersities (PDI > 1.6) were very high, indicating poor control of the polymerization.[13] Moreover, the controllability of polymerizations of MMA in all cases was developed using $FeBr_3$/DPPP as the complex in the absence of any radical initiators or reducing agents.

In addition, the polymerizations of MMA were carried out in toluene at 80 °C using the FeX_3/DPPP (X = Br or Cl) catalyst system initiated by BPN or EBriB. Figure 4a shows kinetics plots of $\ln[M]_0/[M]$ versus time for ATRP of MMA. The polymerizations showed first-order kinetics with respect to the monomer for all initiation systems. Figure 4b shows the dependence of M_n and M_w/M_n on the monomer conversion. The molecular weights of PMMA prepared with the two different iron salts increased linearly with increasing monomer conversion, and the experimental molecular weights followed the theoretical line when $FeBr_3$ was used as the metal salt. Moreover, in the case of the $FeBr_3$/BPN system, the polydispersities (PDI = 1.08 to 1.11) of PMMA were very narrow. The comparison between the initiation systems, $FeBr_3$/initiator, and $FeCl_3$/initiator showed that $FeBr_3$/initiator gave better control of the polymerization, which indicated that the activation/deactivation process was efficient. However, in the case of the $FeCl_3$/EBriB initiation system, the number-average molecular weights were much higher than the theoretical values, indicating that the efficiency of the initiation system was low. The polymerization can be controlled using the $FeCl_3$/DPPP/EBriB system despite the low initiation efficiency given the low polydispersities (PDI = 1.16 to 1.22).

We also examined the effect of monomer-to-initiator concentration on the ATRP of MMA catalyzed by $FeBr_3$/DPPP initiated by EBriB at four different initiator concentrations. The results obtained are shown in Figures 5 and 6. Figure 5 shows the kinetics plots of $\ln[M]_0/[M]$ versus time for the ATRP of MMA. The linear plots demonstrated that the concentration of growing radicals remained constant during the polymerization process. As expected, increasing the initiator concentration led to an enhancement of polymerization rate. In the case of polymerization with a ratio of MMA-to-EBriB of 800:1, the samples could not be withdrawn with a syringe after 6 h because of increasing viscosity. Figure 6 shows the dependence of M_n and M_w/M_n on the monomer conversion in the four different initiator concentrations. The molecular weights of PMMA obtained from all reactions increased linearly with an increase

Table 2. ATRP of MMA in Mixed Toluene/MeOH Solution at 80 °C[a]

entry	$V_{MeOH}/V_{solvent}$ (%)	time (h)	conv (%)	$M_{n,th}$	$M_{n,GPC}$	PDI	k_{app} ($\times 10^{-5}$, s^{-1})
1	0	4	60	14 950	14 050	1.20	6.18
2	5	4	70	14 200	17 000	1.26	7.74
3	10	4	70	14 200	14 250	1.25	8.19
4	20	4	73	14 750	13 550	1.32	8.36
5	30	4	77	15 700	13 900	1.28	11.75
6	40	4	77	15 700	12 800	1.27	12.77
7	60	4	81	16 400	12 600	1.25	13.26

[a] $[MMA]_0 = 4.67$ M; $[MMA]_0/[EBriB]_0/[FeBr_3]_0/[DPPP]_0 = 200:1:1:2$.

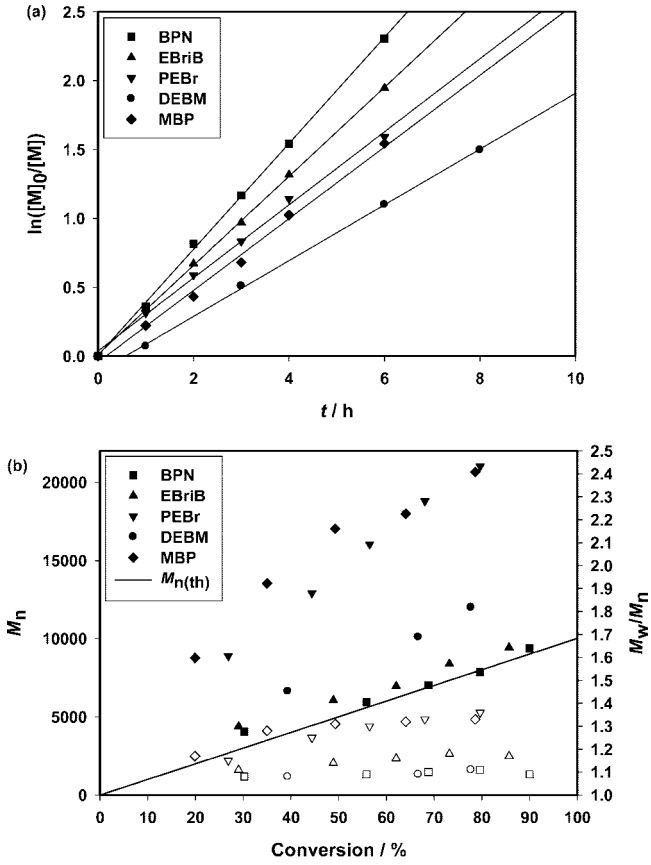

Figure 3. (a) Kinetics plots of $\ln[M]_0/[M]$ versus reaction time and (b) dependence of molecular weights, M_n (filled symbols), and molecular weight distributions, M_w/M_n (open symbols), on the monomer conversion for the ATRP of MMA in toluene with different initiators at 80 °C. $[MMA]_0 = 4.67$ M; $[MMA]_0/[Initiator]_0/[FeBr_3]_0/[DPPP]_0 = 100:1:1:2$.

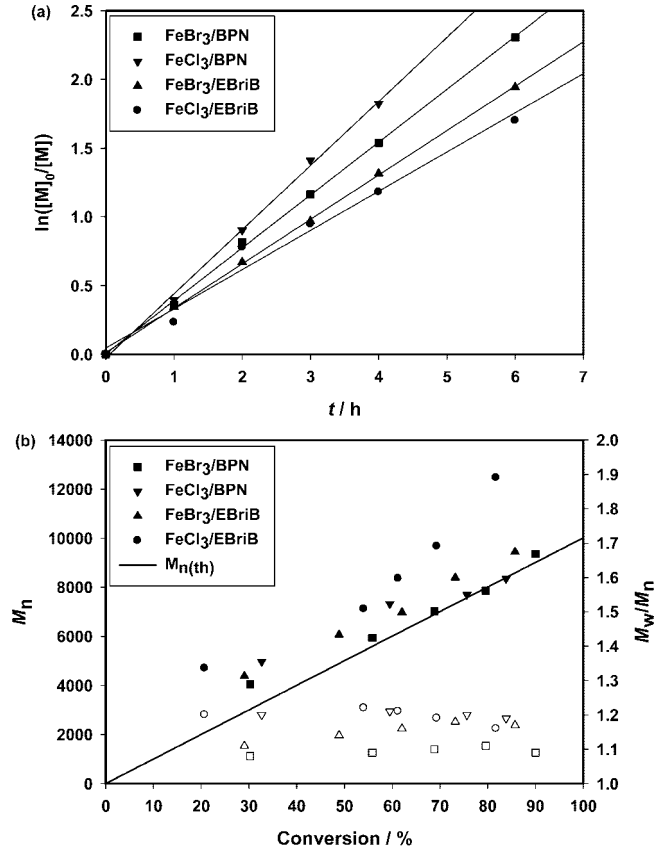

Figure 4. (a) Kinetics plots of $\ln[M]_0/[M]$ versus reaction time and (b) dependence of molecular weights, M_n (filled symbols), and molecular weight distributions, M_w/M_n (open symbols), on the monomer conversion for the ATRP of MMA in toluene with FeX_3/DPPP catalyst system, where X = Br or Cl at 80 °C. $[MMA]_0 = 4.67$ M; $[MMA]_0/[Initiator]_0/[FeX_3]_0/[DPPP]_0 = 100:1:1:2$.

in conversion. A good correlation between the experimental and theoretical molecular weights was achieved for the low ratio of MMA to EBriB. Moreover, the low polydispersities (PDI = 1.10 to 1.20) were observed. It is noteworthy that in the case of 800 ratio of MMA to EBriB, the polymerization of MMA can still be controlled (PDI = 1.16 to 1.28), and the PDIs decreased with increasing monomer conversion (Figure 6b), reaching values of 1.16 at about 55% monomer conversion. Overall, these indicated that the $FeBr_3$/DPPP complex could potentially be used for even higher-molecular-weight PMMA.

Effect of Temperature on ATRP of MMA. In an effort to gain further mechanistic insights, the effect of the reaction temperature on the polymerization was studied in toluene at 60, 80, 90 and 100 °C.

Figure 7 shows the polymerization of MMA at four different temperatures catalyzed by $FeBr_3$ with DPPP as ligand and EBriB as initiator. As shown in Figure 7a, $\ln[M]_0/[M]$ increased linearly with increasing reaction time at all reaction temperatures, suggesting that the radical concentrations in all of these systems were constant. The rate of polymerization increased with increasing temperature. The effect of temperature on the M_n and M_w/M_n values of the PMMA obtained by ATRP is shown in Figure 7b. The experimental molecular weights of PMMA prepared at all of the temperatures used herein increased linearly with increasing monomer conversion and matched the theoretical values very well, indicating that the reaction temperature has little influence on the molecular weights. The molecular weight distributions ($M_w/M_n = 1.10$ to 1.23) were low throughout the polymerization processes. These results illustrated that the

Table 3. Kinetics Data for ATRP of MMA at Different Temperatures[a]

temp (°C)	k_p ($\times 10^3$, mol L^{-1})[b]	k_{app} ($\times 10^{-5}$, s^{-1})[c]	[P•] ($\times 10^{-8}$, mol L^{-1})[d]
60	0.836	3.74	4.47
80	1.320	8.98	6.73
90	1.628	17.25	10.60
100	1.986	34.05	17.15

[a] $[MMA]_0 = 4.67$ M; $[EBriB]_0 = 4.67 \times 10-2$ M. [b] Calculated according to ref 4. [c] Slope of $\ln[M]_0/[M]$ versus time plot. [d] $[P\bullet] = k_{app}/k_p$.

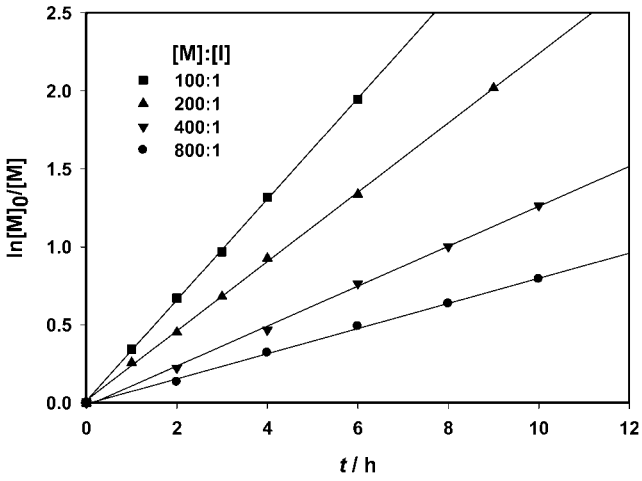

Figure 5. Kinetics plots of $\ln[M]_0/[M]$ versus reaction time for the ATRP of MMA in toluene with different initiator concentrations at 80 °C. $[MMA]_0 = 4.67$ M; $[EBriB]_0/[FeBr_3]_0/[DPPP]_0 = 1:1:2$.

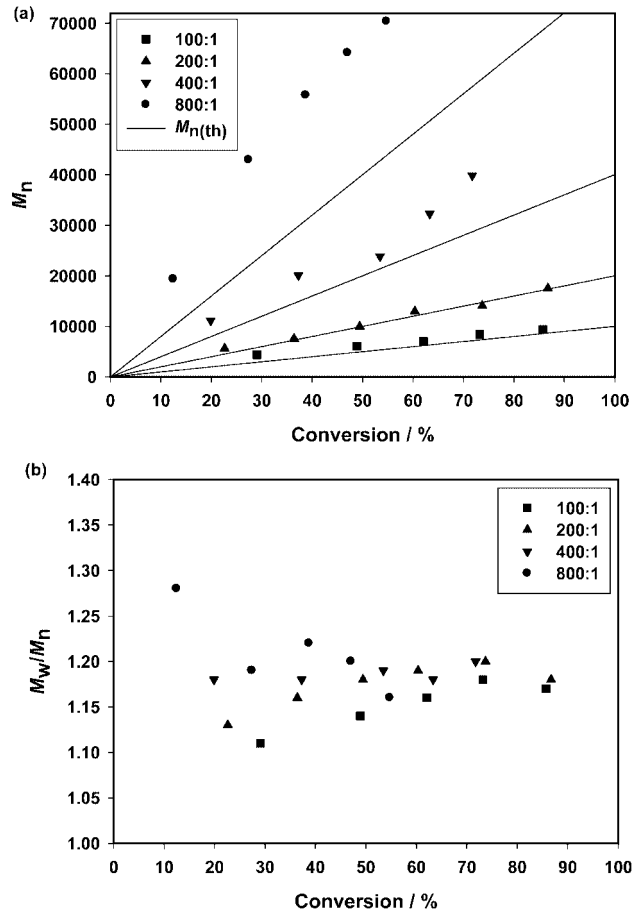

Figure 6. (a) Dependence of molecular weights, M_n, and (b) dependence of molecular weight distributions, M_w/M_n, on the monomer conversion for the ATRP of MMA in toluene with different initiator concentration at 80 °C. $[MMA]_0 = 4.67$ M; $[EBriB]_0/[FeBr_3]_0/[DPPP]_0 = 1:1:2$.

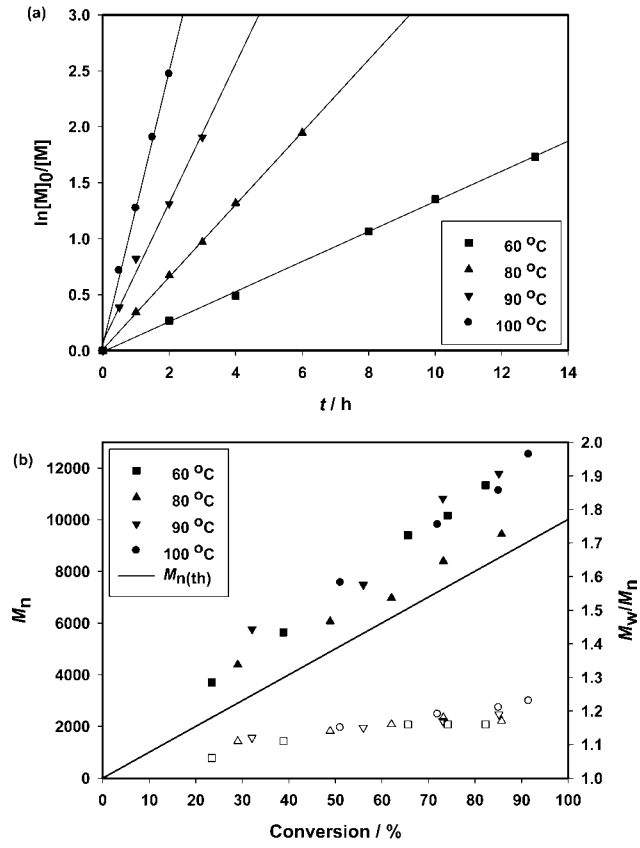

Figure 7. (a) Kinetics plots of $\ln[M]_0/[M]$ versus reaction time and (b) dependence of molecular weights, M_n (filled symbols), and molecular weight distributions, M_w/M_n (open symbols), on the monomer conversion for the ATRP of MMA in toluene at different reaction temperatures. $[MMA]_0 = 4.67$ M; $[MMA]_0/[EBriB]_0/[FeBr_3]_0/[DPPP]_0 = 100:1:1:2$.

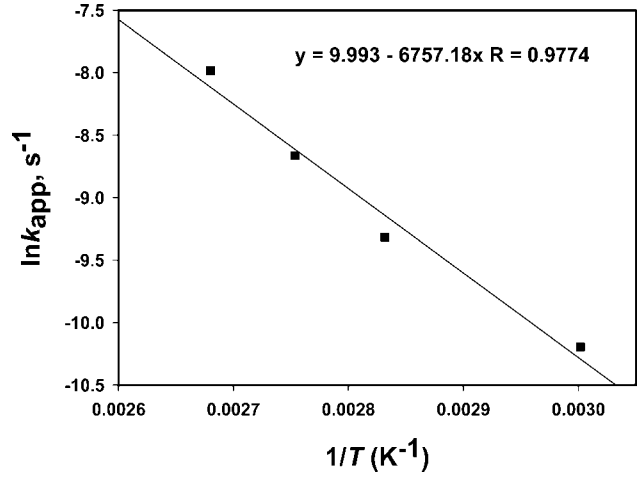

Figure 8. Plot of $\ln k_{app}$ versus $1/T$ for the ATRP of MMA initiated by EBriB in toluene. $[MMA]_0 = 4.67$ M; $[MMA]_0/[EBriB]_0/[FeBr_3]_0/[DPPP]_0 = 100:1:1:2$.

polymerization of MMA mediated by $FeBr_3$/DPPP proceeded via a living process.

The k_{app} values of the polymerizations of MMA at 60, 80, 90, and 100 °C were 3.74×10^{-5}, 8.98×10^{-5}, 17.25×10^{-5}, and 34.05×10^{-5} s^{-1}, respectively. The Arrhenius plot for the $FeBr_3$/DPPP/EBriB-catalyzed polymerization of MMA is shown in Figure 8. On the basis of the slope, the apparent activation energy (E_a) calculated for the initiation system was 56.2 kJ mol^{-1}. Table 3 shows the kinetics data and estimated concentrations of growing radicals in the ATRP of MMA. It is shown that the concentrations of growing radicals increased with increasing polymerization temperature, and the active radical concentrations were much less than the initiator concentration.

ATRP of Styrene. The success of ATRP of MMA with $FeBr_3$/DPPP prompted us to employ the catalyst system for styrene. In the case of ATRPs of MMA, there was no reaction when the ratio of DPPP to $FeBr_3$ was 0:1 (Table 1, entry 15). The styrene polymerization was perfectly inhibited by the

Table 4. Results of ATRPs of Styrene[a]

entry	metal salt	ligand	initiator	time	conv (%)	$M_{n,th}$	$M_{n,GPC}$	PDI
1[b]	$FeBr_3$	none	none	10 s	90[c]		20 500	2.65
2[b]	$FeCl_3$	none	none	30 s	92[c]		31 000	2.32
3	$FeBr_3$	DPPP	PEBr	45 h	62	6600	7000	1.11
4	$FeCl_3$	DPPP	PECl	45 h	31	3300	5300	1.12
5[d]	$FeBr_3$	DPPP	none	24 h	55		7460	1.46
6	$FeBr_2$	DPPP	PEBr	8 h	37	4050	5200	1.42
7	CuBr	DPPP	PEBr	48 h				
8	$CuBr_2$	DPPP	PEBr	48 h				

[a] 110 °C; $[styrene]_0 = 7.25$ M; anisole = 1 mL. [b] Room temperature. [c] From gravimetry. [d] $[styrene]_0 = 7.95$ M; anisole = 0.5 mL.

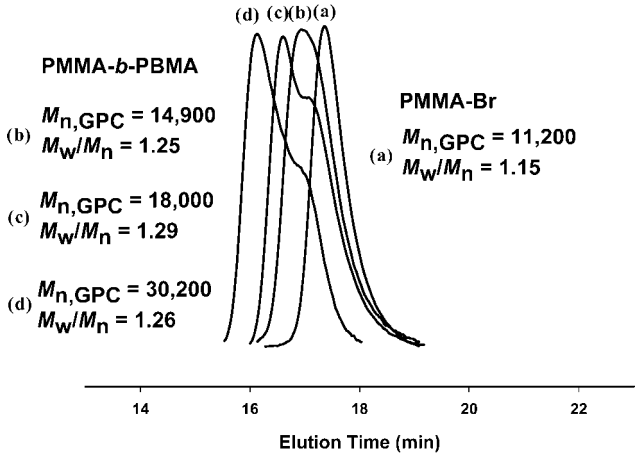

Figure 9. GPC traces of PMMA-*b*-PBMA copolymers obtained in monomer addition experiment with $FeBr_3$/DPPP/EBriB in toluene at 80 °C. $[MMA]_0 = [BMA]_{add} = 2.34$ M; $[MMA]_0/[EBriB]_0/[FeBr_3]_0/[DPPP]_0 = 100:1:1:2$.

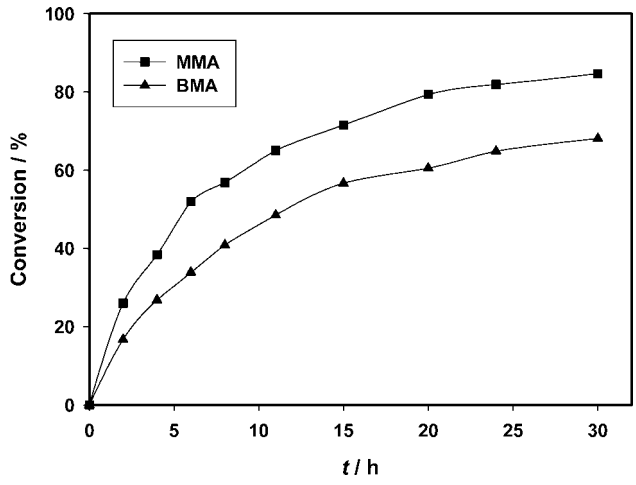

Figure 10. Dependence of the monomer conversion on reaction time for the living random copolymerization of MMA with BMA in toluene at 80 °C. $[MMA]_0 = [BMA]_0 = 2.34$ M; $[MMA]_0/[BMA]_0/[EBriB]_0/[FeBr_3]_0/[DPPP]_0 = 100:100:1:1:2$; $V_{solvents}/V_{monomers} = 1:1$.

addition of a radical scavenger (TEMPO or galvinoxyl), indicating that the iron(III)-catalyzed polymerization of styrene proceeded via a radical mechanism.

Table 4 shows the results of polymerizations of styrene in different catalyst systems. First, the styrene polymerization was carried out using $FeBr_3$ or $FeCl_3$ as catalyst without ligand. The comparison between MMA and styrene polymerization showed that the polymerization of styrene was completed instantaneously to yield polymers with broad molecular weight distributions (Table 4, entries 1 and 2) in the absence of DPPP ligand. The iron(III) halides are common Lewis acids for cationic polymerization. Because of its strong acidity and smaller interaction with a carbonyl compound, iron(III) halide is expected to induce

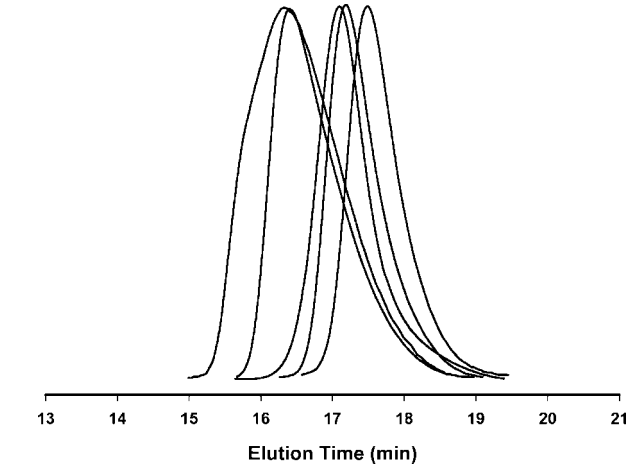

Figure 11. GPC traces of random copolymers (PMMA-*co*-PBMA).

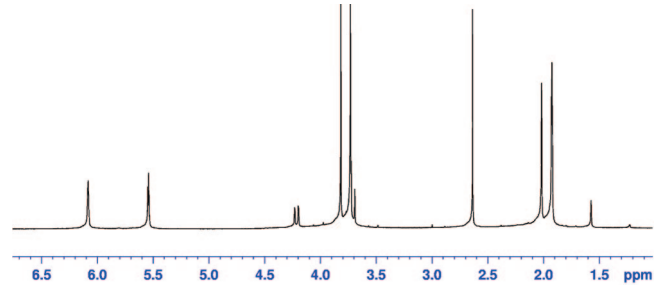

Figure 12. ^1H NMR spectrum ($CDCl_3$) of the product generated by the addition reaction of MMA and $FeBr_3$.

fast cationic polymerization.[60] However, the styrene polymerizations were controlled well in the presence of DPPP ligand (Table 4, entries 3 and 4). To identify the living characteristic of ATRP of styrene catalyzed by the high-oxidation-state iron salt in the absence any radical initiator or reducing agent further, the same experiment with $FeBr_2$/DPPP as complex was run (Table 4, entry 6). In the case of polymerization with $FeBr_2$/DPPP, the molecular weight was higher than the predicted value, and the PDI was high. In addition, when CuBr or $CuBr_2$ was used as metal, no polymerization was observed, which indicated that the complexes were ineffective catalysts for ATRP of styrene (Table 4, entries 7 and 8).

Preparation of Block Copolymers. *Living Block Copolymerization.* To investigate the living nature of the polymerization of MMA with $FeBr_3$/DPPP further, we prepared a block copolymer by adding a fresh BMA to the polymerization solution after the neatly complete consumption of MMA. The GPC of the copolymers obtained from this study is shown in Figure 9. The resulting copolymers showed an increase in molecular weight. Also, the PDIs maintained a narrow range ($M_w/M_n = 1.25$ to 1.29). The block copolymer has a bimodal distribution, suggesting slow initiation of the second block by the macroinitiator of the first block.

Living Random Copolymerization of MMA and BMA. The living random copolymerization of MMA with an equimolar BMA catalyzed by $FeBr_3$/DPPP was carried out in toluene at 80 °C. Time-conversion plots show faster incorporation of MMA than BMA into the copolymer (Figure 10). The molecular weights increase with conversion, and molecular weights distributions were relatively narrow (PDI = 1.18 to 1.45). These results can be seen from some tailing in GPC traces (Figure 11). The increase in the PDI value from 1.18 to 1.45 is understandable because the Fe(III)-catalyzed ATRP of BMA initiated by EBriB under similar reaction conditions already gave polymers with PDI values of ~1.40, as shown in our previous report.[52]

Mechanistic Considerations. The experimental observation that most of the polymerizations were very well controlled without the external addition of Fe(II) demonstrates that Fe(III)/DPPP is an active catalyst for the remarkable ATRP of MMA in the absence of any free radical initiator or reducing agent. An addition reaction of $CuBr_2$ and MMA, which resulted in a reduction in Cu(II) to Cu(I), was reported by Matyjaszewski et al.[61] The oxidizing power of FeX_3 is well established, even for the oxidation of aromatic C−H bonds,[62,63] and thus it is not surprising that the compounds can transfer halogen to an alkene C=C bond. In this reaction, MMA reduced the higher-oxidation-state metal to a lower one, and the mechanism of polymerization can be explained as a normal ATRP. As a result, the polymerization of MMA was well controlled because of the occurrence of the $FeBr_2$/$FeBr_3$/DPPP catalyst system. The ^{1}H NMR spectrum of the product generated by the addition reaction of MMA and $FeBr_3$ revealed the formation of 1,2-dibromoisobutyrate (Figure 12). First, the polymerization of MMA was carried out using $FeBr_3$/DPPP as complex without initiator in toluene at 80 °C. The reaction was so slow that conversion reached 36% after 30 h (Table 1, entry 16). Importantly, the polymers were obtained from this reaction, which indicated that the polymerization could be initiated by one initiator and Fe(II) obtained from the addition reaction via ATRP mechanism. Similarly, the polymers were obtained from the Fe(III)-catalyzed polymerization of styrene without adding ATRP initiator (Table 4, entry 5). Oxidation of the monomer by $FeBr_3$ should yield a halogenated monomer that serves as initiator; indeed polymerization occurs, with rather low PDI. This shows that only a small fraction of $FeBr_3$ is reduced to $FeBr_2$, generating only a small amount of halogenated monomer. This result is quite consistent with the mechanistic proposal. In addition, the rate of MMA polymerization catalyzed by only the iron(III) complex was slower than that obtained from normal ATRP because of the existence of enough of the deactivator (transition-metal complex in its higher oxidation state). These results are in agreement with the assumption that the activator (transition-metal complex in its lower oxidation state) is generated by the reaction between MMA and high-oxidation-state metal salt, and the indirect generation of activator therefore results in the initiation of the ATRP of MMA. Moreover, the radicals are most likely generated through the normal ATRP. The polymerizations of MMA with high-oxidation-state complexes in the absence of any additives are similar to AGET ATRP, whereby the MMA reduces the transition-metal complex in its oxidatively stable state to the activator. To obtain more information about the mechanism of polymerization of MMA initiated by $FeBr_3$/DPPP/EBriB, a radical scavenger (TEMPO or galvinoxyl) was added to the reaction system after 1 h (conversion = 22%). After 9 h, the molecular weights were not changed, and molecular weight distributions remained narrow, which indicated that the polymerization was immediately terminated by the radical scavengers. Therefore, the Fe(III)-catalyzed polymerization of MMA proceeded via a radical mechanism.

Conclusions

A new method for conducting the iron(III)-mediated living polymerization in the absence of any radical initiator or reducing agent was successfully developed, and it proceeds via a radical mechanism indicated by the addition of radical scavengers. The pyridylphosphine ligand, DPPP, was successfully employed in the iron(III)-mediated ATRP, whereby the rate of polymerization attained a maximum at a ligand-to-metal ratio of 2:1 in toluene at 80 °C. The toluene and *p*-xylene solution polymerizations of MMA showed better controllability. Controlled polymerizations of MMA were also observed in methanolic solutions. With EBriB or BPN as initiator, the polymerizations of MMA catalyzed by $FeBr_3$/DPPP under various reaction conditions studied in this article were controlled well. The controlled nature of the polymerization was confirmed by the monomer addition experiment and the block copolymerization. The ATRPs of styrene were successfully performed using $FeBr_2$/DPPP or $FeBr_3$/DPPP as catalyst. Further studies are now in process to explore the new catalyst systems for polymerizing different monomers.

Acknowledgment. This research was supported by the Korea Ministry of Commerce, Industry, and Energy (grant RTI04-01-04, Regional Technology Innovation Program).

References and Notes

(1) Kato, M.; Kamigaito, M.; Sawamoto, M.; Higashimura, T. *Macromolecules* **1995**, *28*, 1721–1723.
(2) Wang, J. S.; Matyjaszewski, K. *J. Am. Chem. Soc.* **1995**, *117*, 5614–5615.
(3) Kamigaito, M.; Ando, T.; Sawamoto, M. *Chem. Rev.* **2001**, *101*, 3689–3746.
(4) Matyjaszewski, K.; Xia, J. *Chem. Rev.* **2001**, *101*, 2921–2990.
(5) Pintauer, T.; Matyjaszewski, K. *Coord. Chem. Rev.* **2005**, *249*, 1155–1184.
(6) Tsarevsky, N. V.; Matyjaszewski, K. *Chem. Rev.* **2007**, *107*, 2270–2299.
(7) Braunecker, W. A.; Matyjaszewski, K. *Prog. Polym. Sci.* **2007**, *32*, 93–146.
(8) Matyjaszewski, K. *Chem.—Eur. J.* **1999**, *5*, 3095–3102.
(9) Jakubowski, W.; Matyjaszewski, K. *Angew. Chem., Int. Ed.* **2006**, *45*, 4482–4486.
(10) Braunecker, W. A.; Matyjaszewski, K. *J. Mol. Catal. A: Chem.* **2006**, *254*, 155–164.
(11) Ando, T.; Kamigaito, M.; Sawamoto, M. *Macromolecules* **1997**, *30*, 4507–4510.
(12) Uchiike, C.; Terashima, T.; Ouchi, M.; Ando, T.; Kamigaito, M.; Sawamoto, M. *Macromolecules* **2007**, *40*, 8658–8662.
(13) Xue, Z.; Lee, B. W.; Noh, S. K.; Lyoo, W. S. *Polymer* **2007**, *48*, 4704–4714.
(14) Xue, Z.; Noh, S. K.; Lyoo, W. S. *J. Polym. Sci., Part A: Polym. Chem.* **2008**, *46*, 2922–2935.
(15) Gibson, V. C.; O'Reilly, R. K.; Wass, D. F.; White, A. J. P.; Williams, D. J. *Macromolecules* **2003**, *36*, 2591–2593.
(16) O'Reilly, R. K.; Shaver, M. P.; Gibson, V. C.; White, A. J. P. *Macromolecules* **2007**, *40*, 7441–7452.
(17) Göbelt, B.; Matyjaszewski, K. *Macromol. Chem. Phys.* **2000**, *201*, 1619–1624.
(18) O'Reilly, R. K.; Gibson, V. C.; White, A. J. P.; Williams, D. J. *Polyhedron* **2004**, *23*, 2921–2928.
(19) Wang, G.; Zhu, X. L.; Zhu, J.; Cheng, Z. P. *J. Polym. Sci., Part A: Polym. Chem.* **2006**, *44*, 483–489.
(20) O'Reilly, R. K.; Gibson, V. C.; White, A. J. P.; Williams, D. J. *J. Am. Chem. Soc.* **2003**, *125*, 8450–8451.
(21) Ibrahim, K.; Yliheikkilä, K.; Abu-Surrah, A.; Löfgren, B.; Lappalainen, K.; Leskelä, M.; Repo, T.; Seppälä, J. *Eur. Polym. J.* **2004**, *40*, 1095–1104.
(22) Cao, J.; Chen, J.; Zhang, K. D.; Shen, Q.; Zhang, Y. *Appl. Catal., A* **2006**, *311*, 76–78.
(23) Niibayashi, S.; Hayakawa, H.; Jin, R. H.; Nagashima, H. *Chem. Commun.* **2007**, 1855–1857.
(24) Ferro, R.; Milione, S.; Bertolasi, V.; Capacchione, C.; Grassi, A. *Macromolecules* **2007**, *40*, 8544–8546.
(25) Louie, J.; Grubbs, R. H. *Chem. Commun.* **2000**, 1479–1480.
(26) Teodorescu, M.; Gaynor, S. G.; Matyjaszewski, K. *Macromolecules* **2000**, *33*, 2335–2339.

(27) Zhu, S.; Yan, D.; Zhang, G.; Li, M. *Macromol. Chem. Phys.* **2000**, *201*, 2666–2669.
(28) Onishi, I.; Baek, K.; Kotani, Y.; Kamigaito, M.; Sawamoto, M. *J. Polym. Sci., Part A: Polym. Chem.* **2002**, *40*, 2033–2043.
(29) Simal, F.; Demonceau, A.; Noels, A. F. *Angew. Chem., Int. Ed.* **1999**, *38*, 538–540.
(30) Simal, F.; Delfosse, S.; Demonceau, A.; Noels, A. F.; Denk, K.; Kohl, F. J.; Weskamp, T.; Herrmann, W. A. *Chem.—Eur. J.* **2002**, *8*, 3047–3052.
(31) Hamasaki, S.; Sawauchi, C.; Kamigaito, M.; Sawamoto, M. *J. Polym. Sci., Part A: Polym. Chem.* **2002**, *40*, 617–623.
(32) Ando, T.; Sawauchi, C.; Ouchi, M.; Kamigaito, M.; Sawamoto, M. *J. Polym. Sci., Part A: Polym. Chem.* **2003**, *41*, 3597–3605.
(33) Opstal, T.; Verpoort, F. *Angew. Chem., Int. Ed.* **2003**, *42*, 2876–2879.
(34) Quebatte, L.; Haas, M.; Solari, E.; Scopelliti, R.; Nguyen, Q. T.; Severin, K. *Angew. Chem., Int. Ed.* **2005**, *44*, 1084–088.
(35) Terashima, T.; Ouchi, M.; Ando, T.; Sawauchi, C.; Kamigaito, M.; Sawamoto, M. *J. Polym. Sci., Part A: Polym. Chem.* **2006**, *44*, 4966–4980.
(36) Uegaki, H.; Kamigaito, M.; Sawamoto, M. *J. Polym. Sci., Part A: Polym. Chem.* **1999**, *37*, 3003–3009.
(37) Moineau, G.; Granel, C.; Dubois, Ph.; Jérôme, R.; Teyssié, Ph. *Macromolecules* **1998**, *31*, 542–544.
(38) Kaneyoshi, H.; Matyjaszewski, K. *Macromolecules* **2005**, *38*, 8163–8169.
(39) Brandts, J. A. M.; van de Geijn, P.; van Faassen, E. E.; Boersma, J.; van Koten, G. *J. Organomet. Chem.* **1999**, *584*, 246–253.
(40) Braunecker, W. A.; Brown, W. C.; Morelli, B. C.; Tang, W.; Poli, R.; Matyjaszewski, K. *Macromolecules* **2007**, *40*, 8576–8585.
(41) Poli, R.; Stoffelbach, F.; Maria, S.; Mata, J. *Chem.—Eur. J.* **2005**, *11*, 2537–2548.
(42) Maria, S.; Kaneyoshi, H.; Matyjaszewski, K.; Poli, R. *Chem.—Eur. J.* **2007**, *13*, 2480–2092.
(43) Zhang, H.; Schubert, U. S. *J. Polym. Sci., Part A: Polym. Chem.* **2004**, *42*, 4882–4894.
(44) Becer, C. R.; Hoogenboom, R.; Fournier, D.; Schubert, U. S. *Macromol. Rapid Commun.* **2007**, *28*, 1161–1166.
(45) Wang, J. S.; Matyjaszewski, K. *Macromolecules* **1995**, *28*, 7572–7573.
(46) Xia, J.; Matyjaszewski, K. *Macromolecules* **1997**, *30*, 7692–7696.
(47) Xia, J.; Matyjaszewski, K. *Macromolecules* **1999**, *32*, 5199–5202.
(48) Gromada, J.; Matyjaszewski, K. *Macromolecules* **2001**, *34*, 7664–7671.
(49) Jakubowski, W.; Matyjaszewski, K. *Macromolecules* **2005**, *38*, 4139–4146.
(50) Tang, H.; Radosz, M.; Shen, Y. *Macromol. Rapid Commun.* **2006**, *27*, 1127–1131.
(51) Xue, Z.; Nguyen, L.; Noh, S. K.; Lyoo, W. S. *Angew. Chem., Int. Ed.* **2008**, *47*, 6426–6429.
(52) Xue, Z.; Oh, H. S.; Noh, S. K.; Lyoo, W. S. *Macromol. Rapid Commun.* **2008**, *29*, 1887–1894.
(53) Newkome, G. R. *Chem. Rev.* **1993**, *93*, 2067–2089.
(54) Mittal, A.; Sivaram, S. *J. Polym. Sci., Part A: Polym. Chem.* **2005**, *43*, 4996–5008.
(55) Zhu, S. M.; Yan, D. Y. *J. Polym. Sci., Part A: Polym. Chem.* **2000**, *38*, 4308–4314.
(56) Inoue, Y.; Matyjaszewski, K. *Macromolecules* **2003**, *36*, 7432–7438.
(57) Bernhardt, P. V. *J. Am. Chem. Soc.* **1997**, *119*, 771–774.
(58) Nanda, A. K.; Matyjaszewski, K. *Macromolecules* **2003**, *36*, 1487–1493.
(59) Uegaki, H.; Kotani, Y.; Kamigaito, M.; Sawamoto, M. *Macromolecules* **1998**, *31*, 6756–6761.
(60) Hanazawa, A.; Hirabaru, Y.; Kanaoka, S.; Aoshima, S. *J. Polym. Sci., Part A: Polym. Chem.* **2006**, *44*, 5795–5800.
(61) Nanda, A. K.; Hong, S. C.; Matyjaszewski, K. *Macromol. Chem. Phys.* **2003**, *204*, 1151–1159.
(62) Kovacic, P.; Brace, N. O. *J. Am. Chem. Soc.* **1954**, *76*, 5491–5494.
(63) Walker, J. D.; Poli, R. *Inorg. Chem.* **1989**, *28*, 1793–1801.

MA802610A